Energy conservation properties of Ritter solution for idealized dam break flow

BENJAMIN DEWALS (IAHR Member), Associate Professor, *Hydraulics in Environmental and Civil Engineering (HECE), Department ArGEnCo, University of Liege, Liege, Belgium*

Email: b.dewals@ulg.ac.be

MARTIN BRUWIER, PhD Researcher, *Hydraulics in Environmental and Civil Engineering (HECE), Department ArGEnCo, University of Liege, Liege, Belgium*

Email: mbruwier@ulg.ac.be

SÉBASTIEN ERPICUM (IAHR Member), Assistant Professor, *Hydraulics in Environmental and Civil Engineering (HECE), Department ArGEnCo, University of Liege, Liege, Belgium*

Email: s.erpicum@ulg.ac.be

MICHEL PIROTTON, Full Professor, *Hydraulics in Environmental and Civil Engineering (HECE), Department ArGEnCo, University of Liege, Liege, Belgium*

Email: michel.pirotton@ulg.ac.be

PIERRE ARCHAMBEAU, Research Associate, *Hydraulics in Environmental and Civil Engineering (HECE), Department ArGEnCo, University of Liege, Liege, Belgium*

Email: pierre.archambeau@ulg.ac.be

Running Head: Energy in Ritter solution

Energy conservation properties of Ritter solution for idealized dam break flow

ABSTRACT

We examine different aspects of energy conservation in the case of the analytical solution of Ritter for idealized dam break flow in a horizontal frictionless and dry channel. We detail the application of the unsteady Bernoulli equation in this case and highlight that the inertial effects cancel out when averaged over the whole flow region. We also show that the potential and kinetic contributions to the total mechanical energy in the flow region have a distinct and constant relative importance: potential energy accounts for 60 %, and kinetic energy for 40 % of the total mechanical energy. These properties of Ritter solution are rarely emphasized while they may be of practical relevance, particularly for the verification of numerical schemes with respect to their ability to ensure energy conservation.

Keywords: Dam break flow; energy conservation; mechanical energy; specific energy; unsteady Bernoulli equation.

1 Introduction

We consider here the case of an idealized dam break flow occurring in a flat and frictionless prismatic channel, with an upstream reservoir of infinite length. The cross-section is rectangular and the initial water depth in the reservoir is noted h_0 (Fig. 1). This idealized configuration also schematizes sudden flow releases resulting from sluice gate operation or hydroelectric load acceptance in a headrace (Sturm, 2010). It was widely used to verify numerical schemes (e.g., Begnudelli & Sanders, 2006; Canelas et al., 2013; Mignot & Cienfuegos, 2009; Oertel & Bung, 2012; Wu, 2008), to compare with experimental data (e.g., El Kadi Abderrezzak et al., 2008; Hsu et al., 2014; Lauber & Hager, 1998a, 1998b; Oertel & Bung, 2012) and to derive more advanced analytical solutions, accounting for flow resistance, initial water depth downstream or bed slope (e.g., Aureli et al., 2014; Chanson, 2009).

Assuming a uniform velocity profile over the flow depth and considering that the pressure distribution is hydrostatic, Ritter (1892) developed an analytical solution based on the theory of characteristics applied to simple wave problems. As shown in Fig. 1, it corresponds to a rarefaction wave (e.g., Rhee et al., 1986) travelling towards upstream in the reservoir, at the velocity $c_0 = (g\ h_0)^{0.5}$, and towards downstream at the velocity - 2 c_0, where g is the gravity acceleration. In the flow region (i.e. - 2 $c_0\ t \leq x \leq c_0\ t$), the water depth h and the depth-averaged flow velocity u may be expressed as a function of time $t > 0$ and position x as (Ritter, 1892):

$$h = \frac{1}{9} h_0 \left(\frac{x}{c_0 t} + 2 \right)^2 , \tag{1}$$

$$u = \frac{2}{3} c_0 \left(\frac{x}{c_0 t} - 1 \right). \tag{2}$$

At the initial location of the dam (x = 0), the water depth is constant (4/9 h_0) and the flow is critical (i.e. F = 1, with $\mathsf{F} = |u|/(gh)^{0.5}$).

As the bottom is assumed frictionless and the flow is continuous, no head losses are encountered in such a flow. We detail here how the conservation of energy can be formulated for this idealized dam break flow configuration. In section 2, we focus on the specific energy, while the conservation of mechanical energy in the flow is examined in section 3.

2 Specific energy

In general, the *energy head* (or *total head*) E is defined as the sum of the elevation z (representing the *potential head*), the *pressure head* $p / (\rho g)$ and the *velocity head* $u^2 / (2 g)$: $E = z + p / (\rho g) + u^2 / (2 g)$, with p the pressure and ρ the fluid density (Chaudhry, 1993; Sturm, 2010). Since the pressure is assumed hydrostatic and the channel bottom is horizontal (z = 0), the sum of potential and pressure heads yields simply the flow depth h, which represents here the *piezometric head*. Hence, the energy head is also equal to the *specific energy* $H = h + u^2 / (2 g)$ (Hager, 2010; Sturm, 2010).

From Eqs. (1) and (2), the *specific energy* H of the flow may be evaluated as a function of position x and time t:

$$H = h + \frac{u^2}{2g} = h_0 \frac{1}{3} \left[\left(\frac{x}{c_0 t} \right)^2 + 2 \right] \tag{3}$$

Although the flow does not lead to *head losses*, the specific energy is obviously neither constant nor uniform. This results from the transient nature of the flow. In particular, H is found minimum (H = 2/3 h_0) at the initial location of the dam (x = 0), where the flow is critical (Fig. 1).

The equation of motion for unsteady flow (e.g., Eq. 7.15 in Sturm, 2010) writes:

$$\frac{1}{g} \frac{\partial u}{\partial t} + \frac{\partial}{\partial x} \left(\frac{u^2}{2g} + h \right) = 0 , \tag{4}$$

in which the non-homogeneous terms (bottom and friction slopes) were omitted since a flat and frictionless bottom is assumed. By integrating Eq. (4) between two arbitrary positions x_A and x_B in the flow region, one obtains:

$$H_A = H_B + \int_{x_A}^{x_B} \frac{1}{g}\frac{\partial u}{\partial t}\,\mathrm{d}x\,, \tag{5}$$

which is one formulation of the unsteady Bernoulli equation.

Given Eq. (2), the inertial term in Eq. (5) becomes:

$$\int_{x_A}^{x_B} \frac{1}{g}\frac{\partial u}{\partial t}\,\mathrm{d}x = -\frac{2}{3}h_0 \int_{x_A/(c_0 t)}^{x_B/(c_0 t)} \xi\,\mathrm{d}\xi = \frac{1}{3}h_0\left[\left(\frac{x_A}{c_0 t}\right)^2 - \left(\frac{x_B}{c_0 t}\right)^2\right]. \tag{6}$$

Introducing Eqs (3) and (6) into Eq. (5) confirms that both sides of Eq. (5) are equal, which follows simply from the fact that the unsteady Bernoulli equation holds for Ritter solution. This is consistent with the absence of head losses under such frictionless and continuous flow conditions.

Integrating the inertial term (6) between the upstream ($x = c_0\,t$) and downstream ($x = -\,2\,c_0\,t$) ends of the flow region, considering $x_A = c_0\,t$ (upstream limit of the flow region), leads to:

$$\int_{-2c_0 t}^{c_0 t} \frac{1}{3}h_0\left[\left(\frac{c_0 t}{c_0 t}\right)^2 - \left(\frac{x}{c_0 t}\right)^2\right]\mathrm{d}x = \frac{1}{3}h_0 c_0 t\int_{-2}^{1}\left(1-\xi^2\right)\mathrm{d}\xi = 0\,. \tag{7}$$

This confirms that the effect of inertia over the whole flow region is to spatially redistribute the specific energy. This contrasts with a standard head loss term, the integral of which would be non-zero.

Consequently, integrating the specific energy over the whole flow domain and up to a finite abscissa L_R in the undisturbed part of the upstream reservoir ($L_R \geq c_0 t$) yields:

$$\int_{-\infty}^{L_R}\left(h + \frac{u^2}{2g}\right)\mathrm{d}x = \underbrace{\int_{-2c_0 t}^{c_0 t} h\,\mathrm{d}x}_{①} + \underbrace{\int_{-2c_0 t}^{c_0 t}\frac{u^2}{2g}\,\mathrm{d}x}_{②} + h_0\left(L_R - c_0 t\right) = h_0\left(2c_0 t + L_R\right), \tag{8}$$

which simply equals the length of the flow domain times the initial specific energy h_0. This is consistent with the fact that inertial effects cancel *in average*. In Eq. (8), term ① represents the streamwise-integration over the flow region of the combination of pressure and potential heads (i.e. piezometric head), while term ② corresponds to the streamwise integration of the velocity head. Their respective values are:

$$① = \int_{-2c_0 t}^{c_0 t} h\,\mathrm{d}x = h_0 c_0 t\frac{1}{9}\int_{-2}^{1}\left(\xi+2\right)^2\,\mathrm{d}\xi = h_0 c_0 t\,, \tag{9}$$

$$② = \int_{-2c_0 t}^{c_0 t}\frac{u^2}{2g}\,\mathrm{d}x = h_0 c_0 t\frac{1}{2}\frac{4}{9}\int_{-2}^{1}\left(\xi-1\right)^2\,\mathrm{d}\xi = 2\,h_0 c_0 t\,, \tag{10}$$

which shows that the piezometric head accounts for 1 / 3 of the streamwise-integrated specific energy over the flow region (3 h_0 c_0 t), while the velocity head contributes for 2 / 3. This ratio remains constant over time as a result of the self-similar nature of Ritter solution.

Since Eq. (4) is derived from the principle of *momentum* conservation, Eq. (8) is not a direct expression of the conservation of the mechanical *energy*. This is discussed in the next section.

3 Mechanical energy

The mechanical energy e per unit mass of a flowing fluid can be expressed as the sum of the *kinetic energy* $v^2 / 2$ and the *potential energy* $g\,z$, both per unit mass (Potter et al., 2010; White, 2008):

$$e = \frac{v^2}{2} + gz\,, \tag{11}$$

with $v = (\boldsymbol{v} \bullet \boldsymbol{v})^{0.5}$, $\boldsymbol{v}$ the fluid velocity vector, measured with respect to a fixed reference frame, and z the vertical elevation above the horizontal channel bottom. Other types of energy, including internal energy, are not considered here as we focus on the motion of an incompressible and inviscid fluid without thermal effects. Under these assumptions, the conservation equation for mechanical energy over an *arbitrary* control volume Ω bounded by a closed surface S writes (Potter et al., 2010):

$$\frac{\partial}{\partial t}\int_{\Omega} \rho\left(gz + \frac{v^2}{2}\right) \mathrm{d}\Omega + \int_{S} \rho\left(gz + \frac{v^2}{2}\right)(\boldsymbol{v} - \boldsymbol{v_I}) \cdot \boldsymbol{n}\, \mathrm{d}S = \int_{S} -p(\boldsymbol{v} \cdot \boldsymbol{n})\, \mathrm{d}S\,, \tag{12}$$

with $\boldsymbol{n}$ the unit vector normal to S pointing outwards and $\boldsymbol{v_I}$ the local velocity of the closed surface S. The shear stress tensor was neglected in Eq. (12) as the fluid is assumed inviscid. The right-hand-side of Eq. (12) represents the power developed by the pressure forces.

Consistently with Ritter solution, we consider a one-dimensional flow domain of unit width, in which only the x-component of the fluid velocity is non-zero, i.e. $\boldsymbol{v} = [\, u \;\; 0 \;\; 0 \,]^{\mathrm{T}}$. Since the velocity distribution is assumed uniform and the pressure is hydrostatic, Eq. (12) reduces to:

$$\begin{aligned} &\frac{\partial}{\partial t}\int_{x_A}^{x_B} \rho\left(g\frac{h^2}{2} + h\frac{u^2}{2}\right) \mathrm{d}x + \rho\left(g\frac{h^2}{2} + h\frac{u^2}{2}\right)_{x=x_B} \left[u(x_B,t) - v_B(t)\right] \\ &-\rho\left(g\frac{h^2}{2} + h\frac{u^2}{2}\right)_{x=x_A} \left[u(x_A,t) - v_A(t)\right] = -\rho g\left[\left(\frac{h^2}{2}\right)_{x=x_B} u(x_B,t) - \left(\frac{h^2}{2}\right)_{x=x_A} u(x_A,t)\right] \end{aligned} \tag{13}$$

where the abscissa x_A and x_B define the positions of two arbitrary cross-sections A and B in the

flow domain. These cross-sections A and B may be mobile, at velocities v_A and v_B respectively. We examine hereafter the application of Eq. (13), first to the flow *region*, next to the whole flow *domain*.

Let us consider first a deforming control volume which expands over time to match the flow region ($-2\,c_0\,t \le x \le c_0\,t$). The first term of the left-hand side in Eq. (13) becomes:

$$\int_{-2c_0t}^{c_0t} \rho\left(g\frac{h^2}{2}+h\frac{u^2}{2}\right)\mathrm{d}x = \rho g\frac{h_0^2}{2}c_0t\underbrace{\frac{1}{81}\int_{-2}^{1}(\xi+2)^4\,\mathrm{d}\xi}_{①}+\rho g\frac{h_0^2}{2}c_0t\underbrace{\frac{4}{81}\int_{-2}^{1}(\xi+2)^2(\xi-1)^2\,\mathrm{d}\xi}_{②}$$
$$= \rho g\frac{h_0^2}{2}c_0t \qquad (14)$$

This confirms that, at any time $t > 0$, the total mechanical energy contained within the flow region is equal to the mean potential energy per unit mass $\rho\,g\,h_0 / 2$ times the volume $h_0\,c_0\,t$ of the undisturbed fluid initially present in the flow region (i.e. between the location of the dam and the upstream position of the rarefaction wave at current time t). In addition, the integrals ① and ② in Eq. (14) are respectively equal to 3 / 5 and 2 / 5. This reveals that the relative contributions of the potential energy and the kinetic energy remain distinctively constant over time, corresponding respectively to 60 % and 40 % of the total energy contained in the flow region. This independence from time results also from the self-similar nature of Ritter solution over time. This is also shown in Fig. 2, which represents the distribution of both contributions over the flow region. The part of the flow region situated downstream of the reservoir (i.e. $x < 0$) contributes predominantly with kinetic energy, while the potential energy dominates within the reservoir (i.e. $x > 0$).

Considering $x_A = -2\,c_0\,t$ and $x_B = c_0\,t$, the right-hand side of Eq. (13) vanishes since $u(x_B,t) = 0$ and $h(x_A,t) = 0$. Given that $v_A(t) = u(x_A,t)$ and taking into account Eq. (14), Eq. (13) yields:

$$\frac{\partial}{\partial t}\left(\rho g\frac{h_0^2}{2}c_0t\right)+\rho g\frac{h_0^2}{2}(-c_0)=0\,, \qquad (15)$$

which is indeed verified as the conservation of energy applies for the smooth and continuous flow conditions considered here. Equation (15) expresses that the rate of change of the total energy contained within the flow region is equal to the potential energy per unit length in the undisturbed part of the reservoir times the celerity c_0 of the rarefaction wave in the reservoir.

Let us consider now a fixed control volume which extends beyond the flow region, from $-\infty$ up to an arbitrary abscissa $L_R \ge c_0\,t$ upstream in the reservoir. Using Eqs. (1) and (2), the volume integral in Eq. (13) may be evaluated as follows:

$$\int_{-\infty}^{L_R} \rho\left(g\frac{h^2}{2}+h\frac{u^2}{2}\right)\mathrm{d}x = \rho g\frac{h_0^2}{2}c_0 t\int_{-2}^{1}\left[\left(\frac{h}{h_0}\right)^2+\frac{h}{h_0}\frac{u^2}{gh_0}\right]\mathrm{d}\left(\frac{x}{c_0 t}\right)+\rho g\frac{h_0^2}{2}\left(L_R-c_0 t\right)=\rho g\frac{h_0^2}{2}L_R\,. \tag{16}$$

This simply results from the fact that, at any time, the total mechanical energy in the flow domain remains equal to the potential energy initially present in the reservoir at rest. Equation (16) is a simple and practical relation which may be used to verify the energy conservation in the discrete solution provided by numerical schemes. Equation (13) holds also for the fixed control volume considered here, since in this case all terms, including the time derivative, are equal to zero.

4 Conclusion

By examining the formulation of energy conservation in the well-known Ritter solution for idealized dam break flow, we highlighted several distinctive properties which are rarely emphasized. The unsteady Bernoulli equation holds with a substantial influence of the inertial term, which nonetheless is zero in average over the *flow length* as inertial effects merely redistribute specific energy. The conservation of mechanical energy in the whole flow domain was also examined. It remains constant over time and equal to its initial value, since the flow is frictionless and continuous. Within the flow region, the relative importance of potential and kinetic energy remains constant over time and takes distinctive values: respectively 60 % and 40 % of the total mechanical energy. Relationships derived here, such as Eq. (16), may prove useful in practice for benchmarking numerical methods in terms of energy conservation.

Acknowledgements

The Authors gratefully acknowledge three anonymous Reviewers and the Associate Editor for their valuable comments.

Funding

This research was partly funded through the ARC grant for Concerted Research Actions, financed by the Wallonia-Brussels Federation.

Notation

$c_0 = (g\,h_0)^{0.5}$ = wave celerity in the undisturbed part of the reservoir (m)

e = mechanical energy per unit mass (m^2s^{-2})

E = energy head (m)

$\mathsf{F} = |u|/(gh)^{0.5}$ = Froude number (-)

g = gravity acceleration (ms^{-2})

h = water depth (m)

H = specific energy (m)

h_0 = initial water depth in the reservoir (m)

L_R = abscissa in the undisturbed part of the upstream reservoir (m)

$\boldsymbol{n}$ = unit vector normal to S and pointing outwards (-)

p = pressure (Pa)

S = closed surface defining the control volume Ω (m^2)

t = time (s)

u = fluid velocity component along direction x (ms^{-1})

$\boldsymbol{v}$ = fluid velocity vector (ms^{-1})

$v = (\boldsymbol{v} \bullet \boldsymbol{v})^{0.5}$ (ms^{-1})

v_A, v_B = velocity of the points A and B (ms^{-1})

$\boldsymbol{v_I}$ = local velocity of the closed surface S (ms^{-1})

x = abscissa along the streamwise direction (m)

x_A, x_B = abscissae at points A and B (m)

z = elevation above the horizontal channel bottom (m)

ρ = fluid density (kg m^{-3})

Ω = arbitrary control volume (m^3)

$\xi = x / (c_0 t)$ = non-dimensional abscissa (-)

References

Aureli, F., Maranzoni, A., & Mignosa, P. (2014). A semi-analytical method for predicting the outflow hydrograph due to dam-break in natural valleys. *Advances in Water Resources, 63*, 38-44. doi: 10.1016/j.advwatres.2013.11.001

Begnudelli, L., & Sanders, B.F. (2006). Unstructured grid finite-volume algorithm for shallow-water flow and scalar transport with wetting and drying. *Journal of Hydraulic Engineering, 132(4),* 371-384. doi: 10.1061/(ASCE)0733-9429(2006)132:4(371)

Canelas, R., Murillo, J., & Ferreira, R.M.L. (2013). Two-dimensional depth-averaged modelling of dam-break flows over mobile beds. *Journal of Hydraulic Research, 51(4),* 392-407. doi: 10.1080/00221686.2013.798891

Chanson, H. (2009). Application of the method of characteristics to the dam break wave problem. *Journal of Hydraulic Research, 47(1),* 41-49. doi: 10.3826/jhr.2009.2865

Chaudhry, H. (1993). *Open-channel flow*. Englewood Cliffs, NJ: Prentice Hall.

El Kadi Abderrezzak, K., Paquier, A., & Gay, B. (2008). One-dimensional numerical modelling of dam-break waves over movable beds: application to experimental and

field cases. *Environmental Fluid Mechanics, 8(2),* 169-198. doi: 10.1007/s10652-008-9056-9

Hager, W. (2010). *Wastewater hydraulics. Theory and practice* (2nd ed.). Heidelberg: Springer.

Hsu, H.-C., Torres-Freyermuth, A., Hsu, T.-J., Hwung, H.-H., & Kuo, P.-C. (2014). On dam-break wave propagation and its implication to sediment erosion. *Journal of Hydraulic Research, 52(2),* 205-218. doi: 10.1080/00221686.2013.857365

Lauber, G., & Hager, W.H. (1998a). Experiments to dambreak wave: horizontal channel. *Journal of Hydraulic Research, 36(3),* 291-306. doi: 10.1080/00221689809498620

Lauber, G., & Hager, W.H. (1998b). Experiments to dambreak wave: sloping channel. *Journal of Hydraulic Research, 36(5),* 761-772. doi: 10.1080/00221689809498601

Mignot, E., & Cienfuegos, R. (2009). On the application of a Boussinesq model to river flows including shocks. *Coastal Engineering, 56(1),* 23-31. doi: 10.1016/j.coastaleng.2008.06.007

Oertel, M., & Bung, D. (2012). Initial stage of two-dimensional dam-break waves: laboratory versus VOF. *Journal of Hydraulic Research, 50(1), 89*-97. doi: 10.1080/00221686.2011.639981

Potter, M.C., Wiggert, D.C., Hondzo, M., Shih, T. I-P., & Chaudhry, K. K. (2010). *Mechanics of fluids* (3rd ed.). Stamford, CT: Cengage Learning.

Rhee, H.K., Aris, R., & Amundson, N.R. (1986). *First order partial differential equations. Theory and applications of single equations, 1*. Englewood Cliffs, NJ: Prentice-Hall.

Ritter, A. (1892). Die Fortpflanzung von Wasserwellen [The propagation of water waves]. *Zeitschrift Verein Deutscher Ingenieure, 36(33),* 947–954 (in German).

Sturm, T. W. (2010). *Open channel hydraulics* (2nd ed.). Boston, MA: McGraw-Hill.

White, F. (2008). *Fluid mechanics* (6th ed.). Boston, MA: McGraw-Hill.

Wu, W. (2008). *Computational river dynamics*. London: Taylor & Francis.

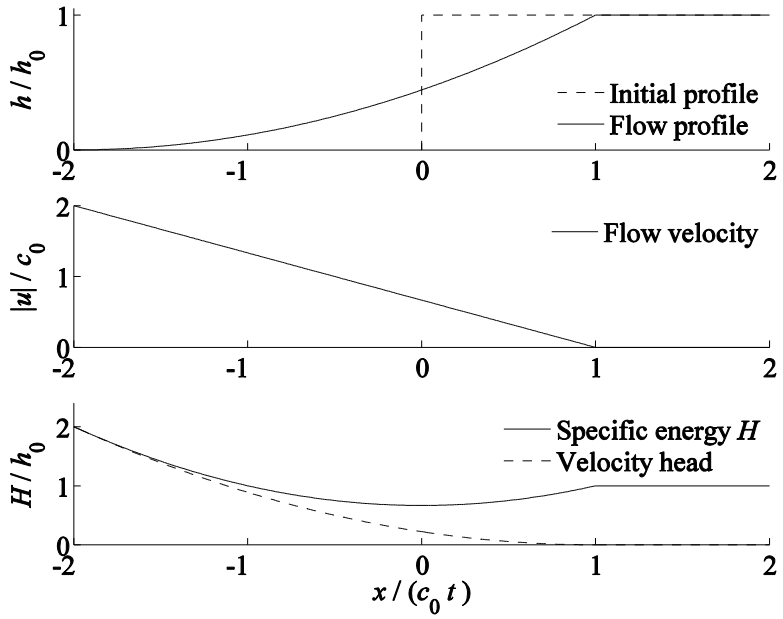

Figure 1 Water depth h, flow velocity u and specific energy H in Ritter solution, normalized using the initial water depth h_0 in the reservoir and the corresponding wave celerity $c_0 = (g\, h_0)^{0.5}$. Flow from right to left.

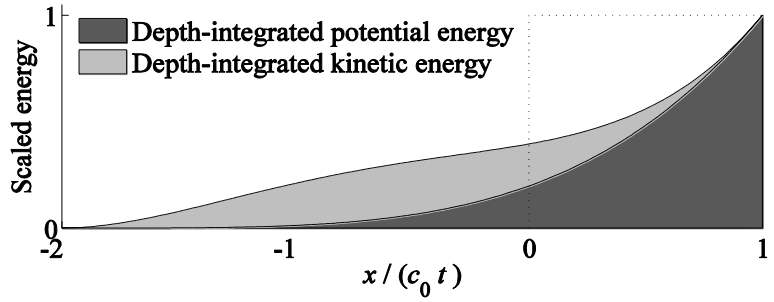

Figure 2 Streamwise distribution of the depth-integrated potential and kinetic energy per unit mass, scaled by the corresponding value $\rho\, g\, h_0^2 / 2$ in the undisturbed part of the reservoir.